

Revisiting a rotating black hole shadow with astrometric observables

Zhe Chang and Qing-Hua Zhu*

*Institute of High Energy Physics, Chinese Academy of Sciences, Beijing 100049, China and
University of Chinese Academy of Sciences, Beijing 100049, China*

(Dated: April 17, 2020)

Abstract

The first image of black hole in M87 galaxy taken by Event Horizon Telescope shows that directed observation of supermassive black holes would be a promising way to test general relativity in strong gravity field regime. In order to calculate shadow of rotating black holes with respect to observers located at finite distance, orthonormal tetrads have been introduced in previous works. However, it is noticed that different choice of tetrads does not lead to the same shape of shadow for observers in near regions. In this paper, we alternatively use formula of astrometric observables for calculating the shadow of a general rotating black hole with respect to these observers. For the sake of intuitive, we also consider Kerr-de Sitter black holes as a representative example. In this space-time, size and shape of Kerr-de Sitter black hole shadows are expressed as functions of distance between the black hole and observer. It is forecasted that the distortion of shadow would increase with distance.

* zhuqh@ihep.ac.cn

I. INTRODUCTION

In strong gravity field regime, one of the most interesting predictions of General relativity might be black holes. Besides existence of stellar-mass black holes nearly to be confirmed by observation of gravitational wave [1], there is also development of directed observation of supermassive black holes in the centre of galaxy, such as the first sketch of black hole in M87 galaxy taken by Event Horizon Telescope (EHT) [2]. And for observation in the future besides the EHT, the *BlackHoleCam* project also targets on making images for Sagittarius A*, the supermassive black hole in the centre of Milky Way [3].

Due to highly bending light rays in strong gravity field, the black holes usually cast a shadow in the view of observers. It has been shown by the first sketch of black hole [2]. What the observers perceive are light rays from unstable circle orbit called photon sphere or photon region. In the sixties of last century, Synge [4] firstly studied the shadow of Schwarzschild black holes. To date, the studies referred to shadow of a spherical black hole are still non-trivial [5–7]. Besides exotic matter and modified gravity [8, 9], one can consider how the expansion rate of the universe would affect size of black hole shadow [10–15]. On the other side, Bardeen [16] firstly shown that the spin of Kerr black holes would cause the shape of shadows distorted. It was originally understood as frame dragging effect on the shadow and expected to be observed in the future [17]. Recent works also considered extended Kerr black holes, such as Kerr-de Sitter black holes [18–20], deformed black holes [21], regular black holes [22, 23], superspinars [24], accelerated Kerr black holes [25], Kerr black holes in the presence of extra dimensions [26, 27] or surrounded by dark matter [28] and Kerr black holes coupled to scalar hair [29, 30], perfect fluid dark matter [31], axion field [32–34], quantized bosonic fields [35] or background vector field [36].

In asymptotic flat space-time, calculation of rotating black hole shadow for distant observers is simple. The formula of angular radius of shadow is the same as that in Minkowski space-time [21–23, 28, 32, 36–42], namely,

$$\alpha_{\text{Dist}} = \lim_{r_o \rightarrow \infty} \left(-r_o \sin \theta_o \left. \frac{d\phi}{dr} \right|_{\theta=\theta_o} \right), \quad (1)$$

$$\beta_{\text{Dist}} = \lim_{r_o \rightarrow \infty} \left(r_o \left. \frac{d\theta}{dr} \right|_{\theta=\theta_o} \right), \quad (2)$$

where (r_o, θ_o) is the position of observer, $\frac{d\phi}{dr}$ and $\frac{d\theta}{dr}$ are used to describe motion of light rays, α_{Dist} and β_{Dist} are angular radius of shadow in two orthonormal directions, approximately.

However, in the presence of a cosmological constant, the non-asymptotic flat space-time does not allow observers located at spatial infinity. And in this case, the Eqs. (1) and (2) would not be valid. To deal with this difficulty, one may introduce orthonormal tetrads for observers located at finite distance. In a pioneer work on Kerr black hole shadow, Bardeen [16] calculated the shape of shadow via introducing orthonormal tetrads with respect to zero-angular-moment-observers (ZAMOs). Recently, this approach has been extended by Stuchlik et al.[19] to calculate shadow of Kerr-de Sitter black holes. Alternatively, Grenzebach et al. [18] firstly used Carter's frame [43] to calculate shadow of Kerr-de Sitter black holes for observers located at finite distance. This approach has also been used in other space-time geometries [31, 44]. Thus, there are mainly two approaches for calculating the shadow of rotating black holes in non-asymptotic flat space-time. The difference is choice of orthonormal tetrads. Unfortunately, the two approaches lead to different shapes of shadow for the observers in near regions.

In this paper, we present a new approach to calculate shadow of rotating black holes for observers located at finite distance without introducing tetrads. The powerful tools we used are astrometric observables, namely, observed angle between two incident light rays in the celestial sphere. We present analytical formulas for shadows of general rotating black holes. Size and shape of Kerr-de Sitter black hole shadow are expressed as functions of distance. For distant observers, our results are consistent with previous works [16, 18]. For observers near the rotating black hole, our results are closed to Grenzebach et al.'s one [18].

This paper is organized as follows. In section II, we utilize formula of astrometric observable to calculate the shadow of spherical black holes. Familiar results of Synge [4] is recovered. In section III, we calculate the shadow of a general rotating black hole in terms of astrometric observables. For given light rays from photon region, we present analytic formula of size and shape of shadows. In section IV, we apply the new approach to Kerr-de Sitter black holes and study how the size and shape of shadow changes with the location of observers. In section V, we compare our results with Bardeen's [16] and Grenzebach et al.'s [18] approaches. Finally, conclusions and discussions are summarised in section VI.

II. ASTROMETRIC OBSERVABLES AND SHADOW OF SPHERICAL BLACK HOLES

It is well known that the directed observable in astrometry is angle between two incident light rays w and k [45, 46],

$$\cos \psi \equiv \frac{\gamma^* w \cdot \gamma^* k}{|\gamma^* w| |\gamma^* k|}, \quad (3)$$

where the inner product is defined by space-time metric $g_{\mu\nu}$ and γ^* is projector for given 4-velocity u , namely $\gamma^*_\nu = \delta_\nu^\mu + u^\mu u_\nu$. We can rewrite Eq. (3) as

$$\cos \psi = \frac{g_{\mu\nu} (\gamma^\mu_\sigma w^\sigma) (\gamma^\nu_\rho k^\rho)}{\sqrt{\gamma_{\alpha\beta} w^\alpha w^\beta} \sqrt{\gamma_{\lambda\kappa} k^\lambda k^\kappa}} = \frac{w \cdot k}{(u \cdot w)(u \cdot k)} + 1, \quad (4)$$

or

$$\cot \psi = \text{sign} \left(\frac{\pi}{2} - \psi \right) \sqrt{-1 - \left(\frac{1}{w \cdot k} \right) \frac{(u \cdot w)^2 (u \cdot k)^2}{(w \cdot k) + 2(u \cdot w)(u \cdot k)}}. \quad (5)$$

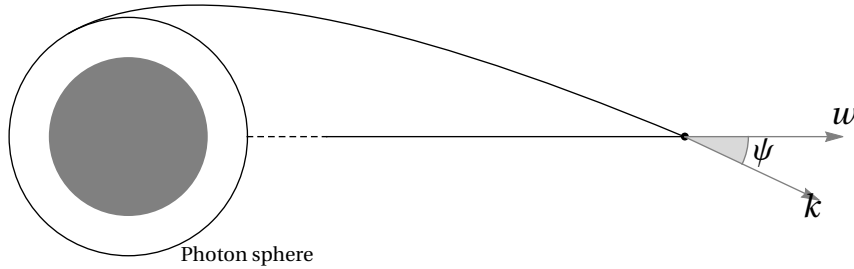


FIG. 1: Schematic diagram of measurement of spherical black hole shadow in astrometry. The ψ is angular radius of shadow. The k is light ray from photon sphere, and w is an auxiliary null vector.

For spherical black holes, the metric can be expressed as

$$ds^2 = g_{00}(dx^0)^2 + g_{11}(dx^1)^2 + g_{22}(dx^2)^2 + g_{33}(dx^3)^2. \quad (6)$$

Here, we would show a general way to calculate size of spherical black hole shadow for static observables, $u = \frac{1}{\sqrt{-g_{00}}} \partial_0$. In the framework of astrometry, schematic diagram is shown in Figure 1. The angular radius of shadow ψ is determined by a straight light ray w from centre of black holes and a bending light ray k from photon sphere. For the radial null geodesic

$w = (w^0, w^1, 0, 0)$ and the observed light ray $k = (k^0, k^1, 0, k^3)$, Eq. (4) becomes as

$$\begin{aligned}\cos \psi &= \frac{g_{00}k^0w^0 + g_{11}k^1w^1}{-g_{00}k^0w^0} + 1 \\ &= \sqrt{-\frac{g_{11}}{g_{00}} \frac{k^1}{k^0}}.\end{aligned}\quad (7)$$

It's consistent with the formula of angular radius of shadow proposed by Cunningham [47] and used in recent Ref. [48]. Additionally, we can rewrite Eq. (7) as

$$\begin{aligned}\cot \psi &= \text{sign} \left(\frac{\pi}{2} - \alpha \right) \sqrt{-1 - \left(\frac{1}{g_{00}k^0w^0 + g_{11}k^1w^1} \right) \frac{(g_{00}k^0w^0)^2}{g_{00}k^0w^0 + g_{11}k^1w^1 - 2g_{00}k^0w^0}} \\ &= \sqrt{\frac{g_{11}}{g_{33}} \frac{k^1}{k^3}}.\end{aligned}\quad (8)$$

It's consistent with the formula proposed by Synge [4] and used in recent Refs. [10, 12]. It shows that Eqs. (7) and (8) in previous works [4, 47] can derive from formula of astrometric observables (Eq. (3)). In the derivation, the straight light ray w functions as an auxiliary null vector. The final results have no relevance with w . The formula of angular radius also can be checked by calculating angular diameter of shadow, which is exactly twice of the angular radius ψ .

On the other side, Eq. (8) can be expressed in terms of orthonormal tetrads $k^{(a)} = e^{(a)}_{\mu} k^{\mu}$, where $e^{(a)}_{\mu} = \text{diag}(\sqrt{-g_{00}}, \sqrt{g_{11}}, \sqrt{g_{22}}, \sqrt{g_{33}})$. From the geometrical intuitive, angular radius should take form of

$$\psi = \cot^{-1} \left(\frac{k^{(1)}}{k^{(3)}} \right).\quad (9)$$

In this sense, the angular radius is angle between light ray k and radial coordinate line.

III. ASTROMETRIC OBSERVABLE FOR SHADOW OF ROTATING BLACK HOLES

For rotating black holes, we can consider a general metric in the form,

$$ds^2 = -g_{00}dt^2 + g_{11}dr^2 + g_{22}d\theta^2 + g_{33}d\phi^2 + 2g_{03}dtd\phi.\quad (10)$$

One might find troubles in understanding angular radius of shadow in terms of orthonormal tetrads with geometrical intuitive. The problem is that non-diagonal component of metric would lead to more than one reasonable choices of orthonormal tetrads, but none of them seems preferred than others.

In the example of Kerr black holes, there are three orthonormal tetrad families, namely, frame of ZAMOs, Carter's frame and static frame [43]. In static frame, the 0-component of tetrad e_0 is along the direction of coordinate time ∂_t . The non-diagonal component of metric would lead to that 4-velocity $p_{(\phi)}$ (in tetrad) and p_ϕ (in coordinate basis ∂_μ) are not in the same direction. Thus, the static frame seems not suited for understanding the angular radius with geometrical intuitive as that for spherical black holes. Maybe, due to this consideration, Bardeen firstly considered the shadow of Kerr black holes with respect to ZAMOs. In this local frame, the 0-component of tetrad e_0 is not adapted to a static observer, while spatial components of 4-velocity $p_{(i)}$ are in the same direction of p_i . It gives a well-understood formulation for angular radius of rotating black hole shadow in the framework of tetrads,

$$\alpha_{\text{Bard}} = - \left. \frac{p_{(\phi)}}{p_{(t)}} \right|_{\text{ZAMO}}, \quad (11)$$

$$\beta_{\text{Bard}} = \left. \frac{p_{(\theta)}}{p_{(t)}} \right|_{\text{ZAMO}}. \quad (12)$$

Carter's frame is fundamentally important to properties of geodesic equations and curvature tensors [43]. Grenzebach et al. [18] firstly used this orthonormal frame to calculate shadow of Kerr-like black holes. However, in near zone from black holes, one might find shapes of Kerr black holes are different with different choice of orthonormal tetrads [16, 18].

In this section, we would alternatively use formula of astrometric observables to calculate shadow of rotating black hole (Eq. (10)). For the sake of intuitive, we consider inclination angle $\theta = 0$ and $\theta = \frac{\pi}{2}$ as representative cases. For rotating black holes, there is not a straight null geodesic as auxiliary vector in general. In the case of $\theta = 0$, we can use the same calculation as that for spherical black hole shadow. While, in the case of $\theta = \frac{\pi}{2}$, we should use geometric trigonometry in celestial sphere.

A. Inclination angle $\theta = 0$

As schematic diagram shown in Figure 2, we consider a straight null curve $w = (w^0, w^0, 0, 0)$ along rotation axis of the rotating black hole and a bending light ray $l = (l^0, l^1, l^2, l^3)$ from photon region. Without spherical symmetric, we can not simply set the third component of light ray $l^2 = 0$. In this case, the angular radius ψ can be given by

Eq. (5),

$$\begin{aligned} \cot \psi &= \text{sign} \left(\frac{\pi}{2} - \psi \right) \sqrt{-1 - \left(\frac{1}{w \cdot l} \right) \frac{(u \cdot w)^2 (u \cdot l)^2}{(w \cdot l) + 2(u \cdot w)(u \cdot l)}} \\ &= \text{sign} \left(\frac{\pi}{2} - \psi \right) \sqrt{\frac{g_{11}}{g_{22} \left(\frac{l^2}{l^1} \right)^2 + \left(g_{33} - \frac{g_{03}^2}{g_{00}} \right) \left(\frac{l^3}{l^1} \right)^2}}. \end{aligned} \quad (13)$$

For $g_{03} = 0$, it reduces to the formula for spherical black holes. One might find that Eq. (13) can not simply read in terms of the tetrads mentioned above [43].

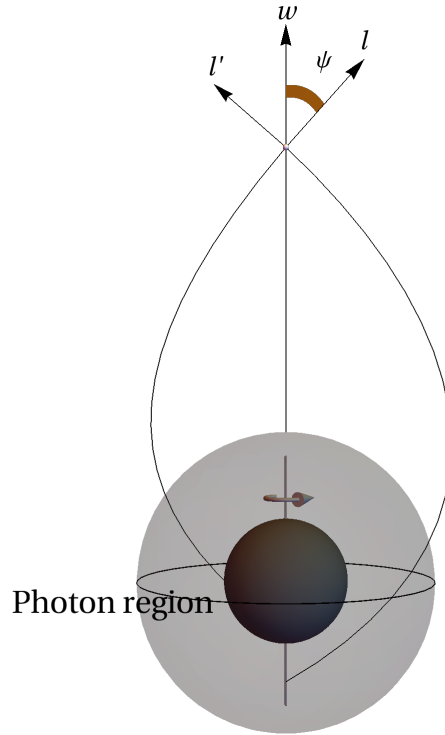


FIG. 2: Schematic diagram of measurement of rotating black hole shadow in astrometry. The observers are located at inclination angle $\theta = 0$. The ψ is angular radius of shadow. The l is light ray from photon region, and w is an auxiliary null vector.

B. Inclination angle $\theta = \frac{\pi}{2}$

In the case of observers located at equatorial plane of a black hole, the calculation of rotating black hole shadows turns to be more tricky. As schematic diagram shown in Figure 3, we consider two bending light rays k and w in the equatorial plane. Due to frame dragging effect, the counter-rotating light ray k has a lower angular velocity than that of light ray w . In astrometry, we can measure the angular distance γ between k and w in the celestial sphere, which is formulated as

$$\begin{aligned}
\cot \gamma &= \text{sgin} \left(\frac{\pi}{2} - \gamma \right) \sqrt{-1 - \left(\frac{1}{k \cdot w} \right) \frac{(u \cdot k)^2 (u \cdot w)^2}{(k \cdot w) + 2(u \cdot k)(u \cdot w)}} \\
&= \text{sign}(k, w) \sqrt{\frac{\left(g_{11} \frac{k^1 w^1}{k^3 w^1 - w^3 k^1} + \left(g_{33} - \frac{g_{03}^2}{g_{00}} \right) \frac{k^3 w^3}{k^3 w^1 - w^3 k^1} \right)^2}{g_{11} \left(g_{33} - \frac{g_{03}^2}{g_{00}} \right)}} \\
&\equiv \text{sign}(k, w) \sqrt{\frac{\left(\frac{g_{11}}{\mathcal{K} - \mathcal{W}} + \left(g_{33} - \frac{g_{03}^2}{g_{00}} \right) \frac{1}{\frac{1}{\mathcal{W}} - \frac{1}{\mathcal{K}}} \right)^2}{g_{11} \left(g_{33} - \frac{g_{03}^2}{g_{00}} \right)}}, \tag{14}
\end{aligned}$$

where $\mathcal{K} \equiv \frac{k^3}{k^1}$, $\mathcal{W} \equiv \frac{w^3}{w^1}$, and

$$\text{sign}(k, w) = \text{sign} \left(g_{11} + \left(g_{33} - \frac{g_{03}^2}{g_{00}} \right) \mathcal{K} \mathcal{W} \right). \tag{15}$$

Because of axisymmetry of rotating black holes, here, we can set $k = (k^0, k^1, 0, k^3)$, $w = (w^0, w^1, 0, w^3)$ for simplicity.

As we known, location in the celestial sphere can be determined by two parameters. For an light ray l from photon region, we determine location of l by parameters α and β . The α is angle between l and k , and the β is angle between l and w . The angular distances α and β can be expressed as

$$\begin{aligned}
\cot \alpha &= \text{sign} \left(\frac{\pi}{2} - \alpha \right) \sqrt{-1 - \left(\frac{1}{k \cdot l} \right) \frac{(u \cdot k)^2 (u \cdot l)^2}{(k \cdot l) + 2(u \cdot k)(u \cdot l)}} \\
&= \text{sign}(k, l) \sqrt{\frac{\left(g_{11} \frac{1}{\mathcal{K} - \mathcal{L}_3} + \left(g_{33} - \frac{g_{03}^2}{g_{00}} \right) \frac{1}{\frac{1}{\mathcal{L}_3} - \frac{1}{\mathcal{K}}} \right)^2}{g_{22} \left(g_{11} \left(\frac{\mathcal{L}_2}{\mathcal{K} - \mathcal{L}_3} \right)^2 + \left(g_{33} - \frac{g_{03}^2}{g_{00}} \right) \left(\frac{\mathcal{L}_2}{1 - \frac{\mathcal{L}_3}{\mathcal{K}}} \right)^2 \right) + g_{11} \left(g_{33} - \frac{g_{03}^2}{g_{00}} \right)}}, \tag{16}
\end{aligned}$$

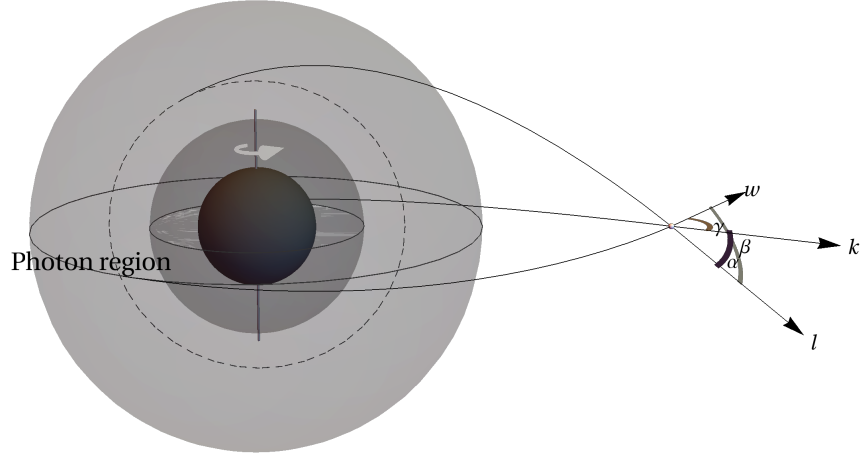


FIG. 3: Schematic diagram of measurement of rotating black hole shadow in astrometry. The observers are located at inclination angle $\theta = \frac{\pi}{2}$. The k , w and l are light rays from photon region. The γ , α , β are angles between k and w , l and k , l and w , respectively.

and

$$\begin{aligned} \cot \beta &= \text{sign} \left(\frac{\pi}{2} - \beta \right) \sqrt{-1 - \left(\frac{1}{w \cdot l} \right) \frac{(u \cdot w)^2 (u \cdot l)^2}{(w \cdot l) + 2(u \cdot w)(u \cdot l)}} \\ &= \text{sign}(w, l) \sqrt{\frac{\left(g_{11} \frac{1}{\mathcal{W} - \mathcal{L}_3} + \left(g_{33} - \frac{g_{03}^2}{g_{00}} \right) \frac{1}{\mathcal{L}_3 - \frac{1}{\mathcal{K}}} \right)^2}{g_{22} \left(g_{11} \left(\frac{\mathcal{L}_2}{\mathcal{W} - \mathcal{L}_3} \right)^2 + \left(g_{33} - \frac{g_{03}^2}{g_{00}} \right) \left(\frac{\mathcal{L}_2}{1 - \frac{\mathcal{L}_3}{\mathcal{W}}} \right)^2 \right) + g_{11} \left(g_{33} - \frac{g_{03}^2}{g_{00}} \right)}}, \quad (17) \end{aligned}$$

where $\mathcal{L}_2 \equiv \frac{l^3}{l}$, $\mathcal{L}_3 \equiv \frac{l^3}{l}$.

In Figure 4, we present schematic diagram for shadow of rotating black holes in view of observers. The boundary of shadow is determined by all the light rays l received by observers. And celestial coordinates (Ψ, Φ) of shadow can be expressed in terms of α , β and

γ ,

$$\cos A = \frac{\cos \alpha - \cos \beta \cos \gamma}{\sin \beta \sin \gamma}, \quad (18)$$

$$\frac{\sin \beta}{\sin \frac{\pi}{2}} = \frac{\sin \left(\frac{\pi}{2} - \Psi \right)}{\sin A}, \quad (19)$$

$$\cos \beta = \cos \left(\frac{\pi}{2} - \Psi \right) \cos(\gamma - \Phi) + \sin \left(\frac{\pi}{2} - \Psi \right) \cos(\gamma - \Phi) \cos \left(\frac{\pi}{2} \right). \quad (20)$$

Then, we have

$$\Psi = \frac{\pi}{2} - \arcsin \left(\sin \beta \sqrt{1 - \left(\frac{\cos \alpha - \cos \beta \cos \gamma}{\sin \beta \sin \gamma} \right)^2} \right), \quad (21)$$

$$\Phi = \gamma - \arccos \left(\frac{\cos \beta}{\cos \left(\frac{\pi}{2} - \Psi \right)} \right). \quad (22)$$

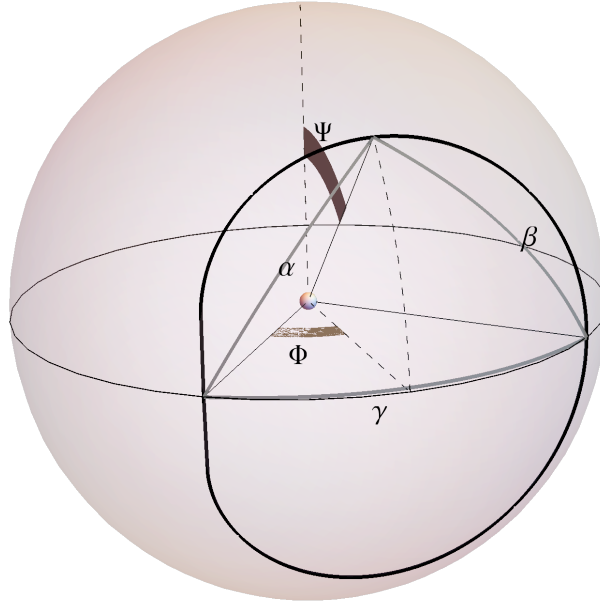


FIG. 4: Schematic diagram for the shadow of rotating black holes in view of observers. The α , β and γ are the angles shown in Figure 3. The Ψ and Φ are the celestial coordinates in the view of observers. The distorted circle in the celestial sphere is the boundary of shadow of a rotating black hole. Here, we use the shadow of Kerr black holes for instance.

The most interesting part of rotating black hole shadow is lying on its shape. Because of frame dragging effect on propagating light rays, the shape of shadow is usually distorted from a circle in the view of observers. In order to describe clearly the shape of shadow in 2D-plane, we use a stereographic projection for the celestial coordinates,

$$Y_{\text{sh}} = \frac{2 \sin \Phi \sin \Psi}{1 + \cos \Phi \sin \Psi} , \quad (23)$$

$$Z_{\text{sh}} = \frac{2 \cos \Psi}{1 + \cos \Phi \sin \Psi} . \quad (24)$$

The schematic diagram for the stereographic projection is presented in Figure 5. As a circle in celestial sphere is mostly projected to a circle on 2D-plane, the shape of shadow beyond a circle in 2D-plane can involve property of space-time beyond spherical black holes.

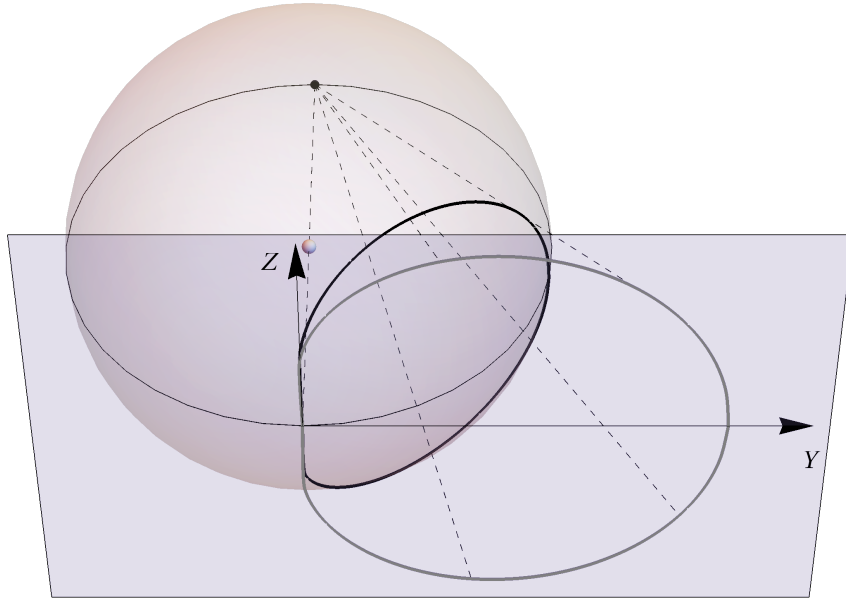


FIG. 5: Schematic diagram for stereographic projection. Here, we use Kerr black holes for instance.

In this section, we calculate shadow of a general rotating black hole by making use of the formula of astrometric observables. In Eqs. (13), (14), (16) and (17) , the light rays k , w and l are moving along null geodesics. And the integral constants of these null vectors are

determined by the photon region of rotating black holes. Thus, for the sake of intuitive, we would apply our formula to Kerr-de Sitter black holes in next section.

IV. APPLICATION IN KERR-DE SITTER BLACK HOLES

The space-time of Kerr-de Sitter black holes is non-asymptotically flat. The calculation of shadow for an observer located at spatial infinity wouldn't be valid any more. By introducing orthonormal tetrads, Grenzebach et al. [18] discussed the shadow for observers fixed in finite distance. In this paper, we also aim at this situation. Without introducing tetrads, we use formula of astrometric observables instead,

The metric of Kerr-de Sitter black holes [18, 31, 49] is given by

$$ds^2 = -\frac{\Delta_r}{I^2\Sigma}(dt - a\sin^2\theta d\phi)^2 + \frac{\Delta_\theta \sin^2\theta}{I^2\Sigma}(adt - (r^2 + a^2)d\phi)^2 + \frac{\Sigma}{\Delta_r}dr^2 + \frac{\Sigma}{\Delta_\theta}d\theta^2, \quad (25)$$

where

$$\Delta_r(r) = -\frac{1}{3}\Lambda r^2(r^2 + a^2) + r^2 - 2Mr + a^2, \quad (26)$$

$$\Delta_\theta(\theta) = 1 + \frac{1}{3}\Lambda a^2 \cos^2\theta, \quad (27)$$

$$I = 1 + \frac{1}{3}\Lambda a^2, \quad (28)$$

$$\Sigma(r, \theta) = r^2 + a^2 \cos^2\theta. \quad (29)$$

The M is black hole mass, a is spin parameter and Λ is cosmological constant. From the metric (Eq. (25)), one can obtain 4-velocities of light rays via Hamiltonian-Jacobi method (see, for example, [16, 18, 31]),

$$\Sigma p^t = I^2 E \left(\frac{(r^2 + a^2 - a\lambda)(r^2 + a^2)}{\Delta_r} + \frac{a(\lambda - a\sin^2\theta)}{\Delta_\theta} \right), \quad (30)$$

$$(\Sigma p^r)^2 = R(r), \quad (31)$$

$$(\Sigma p^\theta)^2 = \Theta(\theta), \quad (32)$$

$$\Sigma p^\phi = I^2 E \left(\frac{a(r^2 + a^2) - a^2\lambda}{\Delta_r} + \frac{\lambda - a\sin^2\theta}{\Delta_\theta \sin^2\theta} \right), \quad (33)$$

where

$$R(r) = E^2(I^2(r^2 + a^2 - a\lambda)^2 - \Delta_r\kappa), \quad (34)$$

$$\Theta(\theta) = E^2 \left(\Delta_\theta\kappa - \frac{I^2(\lambda - a\sin^2\theta)^2}{\sin^2\theta} \right), \quad (35)$$

and

$$\lambda \equiv \frac{L}{E} , \quad (36)$$

$$\kappa \equiv \frac{K}{E^2} . \quad (37)$$

The L, E, K are integral constants from the null geodesic equations. The photon region of Kerr-de Sitter space-time has been studied carefully in Ref. [18]. It's determined by unstable circle orbits formulated as

$$R(r_c) = 0 , \quad (38)$$

$$\left. \frac{dR(r)}{dr} \right|_{r=r_c} = 0 , \quad (39)$$

which lead to

$$\lambda(r_c) = \frac{1}{a} \left(r^2 + a^2 - \frac{4r\Delta_r}{\Delta'_r} \right) \Big|_{r=r_c} , \quad (40)$$

$$\kappa(r_c) = \frac{16I^2 r^2 \Delta_r}{(\Delta'_r)^2} \Big|_{r=r_c} , \quad (41)$$

where r_c is the location of photon region. The range of r_c is determined by $\Theta(\theta) \geq 0$, namely,

$$((4r\Delta_r - \Sigma\Delta'_r)^2 - 16a^2 r^2 \Delta_r \Delta_\theta \sin^2 \theta)_{r=r_c} \leq 0 . \quad (42)$$

Here, r_{c-} and r_{c+} are minimum and maximum radial position of photon region outside of inner horizon. If limiting the null vectors from the photon region, one can regard p^μ as function of x^μ , E and r_c . One should note that θ is a coordinate of observers. As shown in Figure 2 and 3, the photon region is different for different locations of observers.

A. Sizes of shadow

For observers located at inclination angle $\theta = 0$, the Eq. (42) can be rewritten as

$$(4r\Delta_r - (r^2 + a^2)\Delta'_r)_{r=r_c} = 0 . \quad (43)$$

In this case, $r_c = r_{c-} = r_{c+} \equiv r_{c0}$. Using Eq. (13), one can obtain angular radius of Kerr-de Sitter black hole shadow in the form,

$$\cot \psi = \sqrt{\frac{I^2(r^2 + a^2 - a\lambda_0)^2 - \Delta_r \kappa_0}{\lambda_0 a I^2 (2r^2 + 2a^2 - a\lambda_0) + \Delta_r \kappa_0}} , \quad (44)$$

where $\lambda_0 \equiv \lambda(r_{c0})$ and $\kappa_0 \equiv (r_{c0})$. Here, we only consider shadow in the view of observers located outside of the photon region.

In Figure 6. we present the angular radius as function of distance from central black hole. The r_{c0} is smaller than radius of photon sphere of Schwarzschild black holes. In the left panel, it shows that angular radius decreases with spin parameter a . And in the right panel, the angular radius also decreases with cosmological constant Λ . Among these black holes, the size of Schwarzschild black hole shadow is the largest.

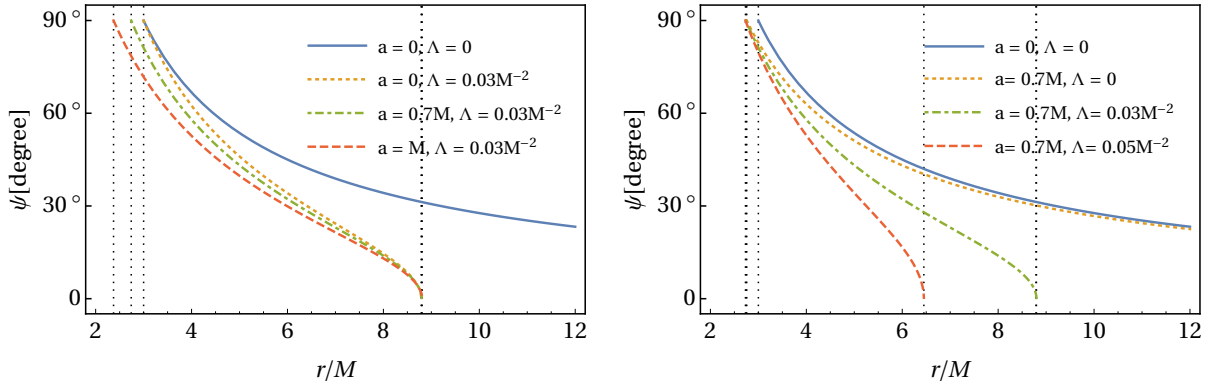


FIG. 6: Angular radius as function of distance from rotating black holes for selected parameters.

The observers are located at inclination angle $\theta = 0$. The vertical dotted lines are outer boundaries and cosmological horizons. Left panel: Angular radius as function of distance for different spin parameters. Right panel: Angular radius as function of distance for different cosmological constants.

For observers located at inclination angle $\theta = \frac{\pi}{2}$, we can determine the range of r_c from Eq. (42), which takes the form of

$$((4r\Delta_r - r^2\Delta_r')^2 - 16a^2r^2\Delta_r)_{r=r_c} \leq 0. \quad (45)$$

Namely, $r_{c-} \leq r_c \leq r_{c+}$. From Eq. (14), we get the angular diameter γ in the Kerr-de space-time,

$$\cot \gamma = \text{sign} \left(1 + \frac{\Delta_r^2}{I^2(\Delta_r - a^2)} \mathcal{KW} \right) \left| \frac{I\sqrt{\Delta_r - a^2}}{\Delta_r} \frac{1}{\mathcal{K} - \mathcal{W}} + \frac{\Delta_r}{I\sqrt{\Delta_r - a^2}} \frac{1}{\frac{1}{\mathcal{W}} - \frac{1}{\mathcal{K}}} \right|, \quad (46)$$

where

$$\mathcal{K} = \left. \frac{p^\phi}{p^r} \right|_{r_c=r_{c-}}, \quad (47)$$

$$\mathcal{W} = \left. \frac{p^\phi}{p^r} \right|_{r_c=r_{c+}}, \quad (48)$$

and

$$\frac{p^\phi}{p^r} = \frac{I^2 \left(\frac{a(r^2+a^2-a\lambda)}{\Delta_r} + \lambda - a \right)}{\sqrt{I^2(r^2+a^2-a\lambda)^2 - \Delta_r \kappa}}. \quad (49)$$

Here, $\frac{p^\phi}{p^r}$ is function of r, r_c .

We plot angular diameter γ as function of distance r in Figure 7. The outer boundary of photon region r_{c+} is larger than radius of photon sphere in Schwarzschild space-time. In the left panel, it shows that the spin parameters hardly affect the angular diameter. The right panel shows that the angular diameter decreases with cosmological constant Λ .

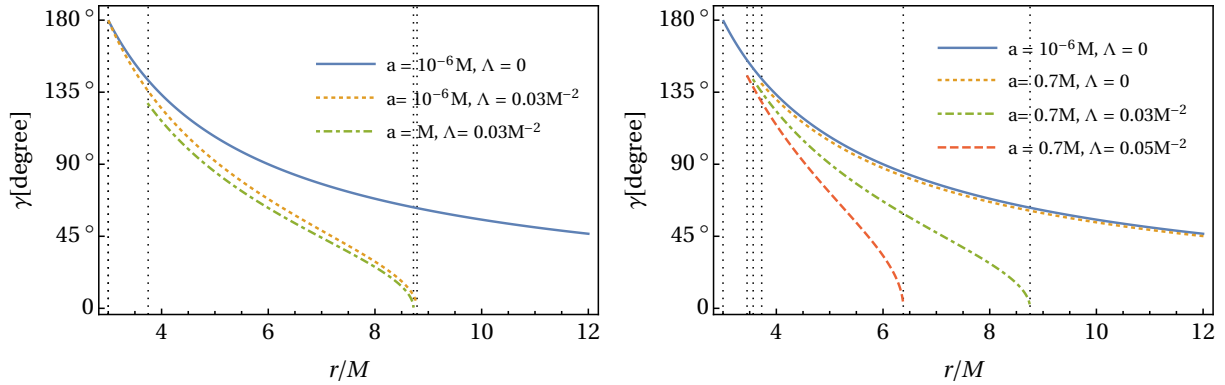


FIG. 7: Angular diameter γ as function of distance from rotating black holes for selected parameters. The observers are located at inclination angle $\theta = \frac{\pi}{2}$. The vertical dotted lines are outer boundaries and cosmological horizons. Left panel: Angular diameter as function of distance for different spin parameters. Right panel: Angular diameter as function of distance for different cosmological constants.

We can conclude that the size of Kerr-de Sitter black hole shadow decreases with spin parameter a and cosmological constant Λ and the shadow of Schwarzschild black hole is the biggest among Kerr-de Sitter black holes.

B. Shapes of shadow

In this part, we turn to shape of Kerr-de Sitter black hole shadow as function of distance. The observers located at inclination angle $\theta = 0$ would see the shadow as a perfect circle, while, the observers located at $\theta = \frac{\pi}{2}$ would find that the shadow is distorted. In this case of Kerr-de Sitter black holes, Eqs. (16) and (17) read

$$\cot \alpha = \text{sign} \left(1 + \frac{\Delta_r^2}{I^2(\Delta_r - a^2)} \mathcal{K} \mathcal{L}_3 \right) \frac{\left| \frac{I\sqrt{\Delta_r - a^2}}{\Delta_r} \frac{1}{\mathcal{K} - \mathcal{L}_3} + \frac{\Delta_r}{I\sqrt{\Delta_r - a^2}} \frac{1}{\frac{1}{\mathcal{L}_3} - \frac{1}{\mathcal{K}}} \right|}{\sqrt{1 + \frac{I^2(\Delta_r - a^2)}{\Delta_r} \left(\frac{\mathcal{L}_2}{\mathcal{K} - \mathcal{L}_3} \right)^2 + \Delta_r \left(\frac{\mathcal{L}_2}{1 - \frac{\mathcal{L}_3}{\mathcal{K}}} \right)^2}}, \quad (50)$$

$$\cot \beta = \text{sign} \left(1 + \frac{\Delta_r^2}{I^2(\Delta_r - a^2)} \mathcal{W} \mathcal{L}_3 \right) \frac{\left| \frac{I\sqrt{\Delta_r - a^2}}{\Delta_r} \frac{1}{\mathcal{W} - \mathcal{L}_3} + \frac{\Delta_r}{I\sqrt{\Delta_r - a^2}} \frac{1}{\frac{1}{\mathcal{L}_3} - \frac{1}{\mathcal{W}}} \right|}{\sqrt{1 + \frac{I^2(\Delta_r - a^2)}{\Delta_r} \left(\frac{\mathcal{L}_2}{\mathcal{W} - \mathcal{L}_3} \right)^2 + \Delta_r \left(\frac{\mathcal{L}_2}{1 - \frac{\mathcal{L}_3}{\mathcal{W}}} \right)^2}}, \quad (51)$$

where \mathcal{W}, \mathcal{K} are given by Eqs. (47), (48) and

$$\mathcal{L}_2 \equiv \left. \frac{p^\theta}{p^r} \right|_{r_c}, \quad (52)$$

$$\mathcal{L}_3 \equiv \left. \frac{p^\phi}{p^r} \right|_{r_c}, \quad (53)$$

and

$$\frac{p^\theta}{p^r} = \pm \sqrt{\frac{\kappa - I^2(\lambda - a)^2}{I^2(r^2 + a^2 - a\lambda)^2 - \Delta_r \kappa}}. \quad (54)$$

The $r_{c-} \leq r_c \leq r_{c+}$, is determined by Eq. (45). In terms of the angular distance α, β and γ , we can give the shape of shadow on the projective plane (X, Y) . Namely, from Eqs. (21)–(24), the boundary of shadow is described by

$$Y_{\text{sh}} = \frac{2 \cos \beta \sin \gamma - 2 \cot \gamma \sqrt{\sin^2 \gamma \sin^2 \beta + (\cos(\beta + \gamma) - \cos \alpha)(\cos(\beta - \gamma) - \cos \alpha)}}{1 + \cos \beta \cos \gamma + \sqrt{\sin^2 \gamma \sin^2 \beta + (\cos(\beta + \gamma) - \cos \alpha)(\cos(\beta - \gamma) - \cos \alpha)}} \quad (55)$$

$$Z_{\text{sh}} = \frac{2 \csc \gamma \sqrt{(\cos \alpha - \cos(\beta + \gamma))(\cos(\beta - \gamma) - \cos \alpha)}}{1 + \cos \beta \cos \gamma + \sqrt{\sin^2 \gamma \sin^2 \beta + (\cos(\beta + \gamma) - \cos \alpha)(\cos(\beta - \gamma) - \cos \alpha)}}. \quad (56)$$

On the projective plane (Y, Z) , the boundary of shadow is described by a parametrized curve in terms of parameter r_c , which has been shown in Figure 5.

In Figure 8, we plot shadow of Kerr(-de Sitter) black holes with selected parameters for distant observers by using Eqs. (55) and (56). In the left panel of Figure 8, the shape of

Kerr black hole shadow seems the same as obtained by previous works [16, 18]. We would present further comparison in next section. As shown in the right panel of Figure 8, the shadow of Kerr-de Sitter black hole seems not serious distorted as spin parameter $a \rightarrow 1$. In Figure 9, we plot shadow of Kerr-de Sitter black holes with selected parameters for observers closed to the black hole. It shows that the spin parameter would cause distortion of shadow, while, cosmological constant could relieve the distortion of the shadow. Besides, the shape of shadow for observers in near region is different from the shape for distant observers. For example, one can compare the shape of shadow for the Kerr black holes with $a = (1 - 10^{-6})M$ in Figures 8 and 9.

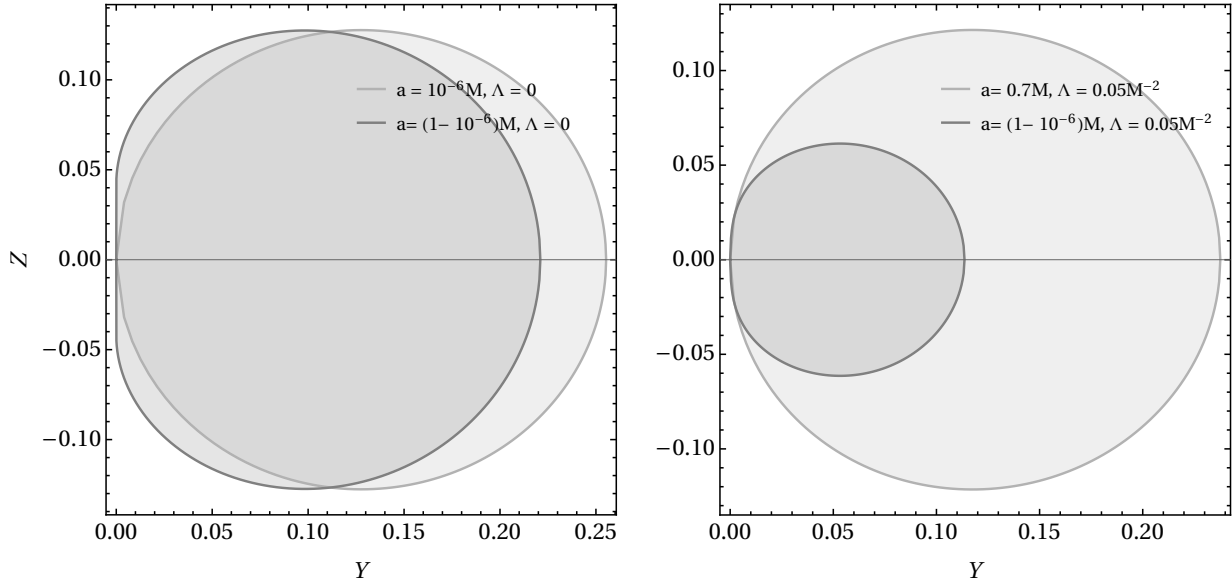


FIG. 8: Shadow of Kerr-de Sitter black holes on projective plane (Y, X) for distant observers.

Left panel: Shadow of Kerr black holes for selected spin parameters for observers located at $r = 40M$. Right panel: Shadow of Kerr-de Sitter black holes with cosmological constant $0.05M^{-2}$ for selected spin parameters for observers located cosmological horizon $r \approx 6.31M$.

For a quantifiable description of the shape of shadow, we could introduce distortion parameter as

$$\delta \equiv 1 - \frac{D_{\min}}{D_{\max}}, \quad (57)$$

where D_{\min} and D_{\max} are largest and smallest diameters of shadow, respectively. This kind

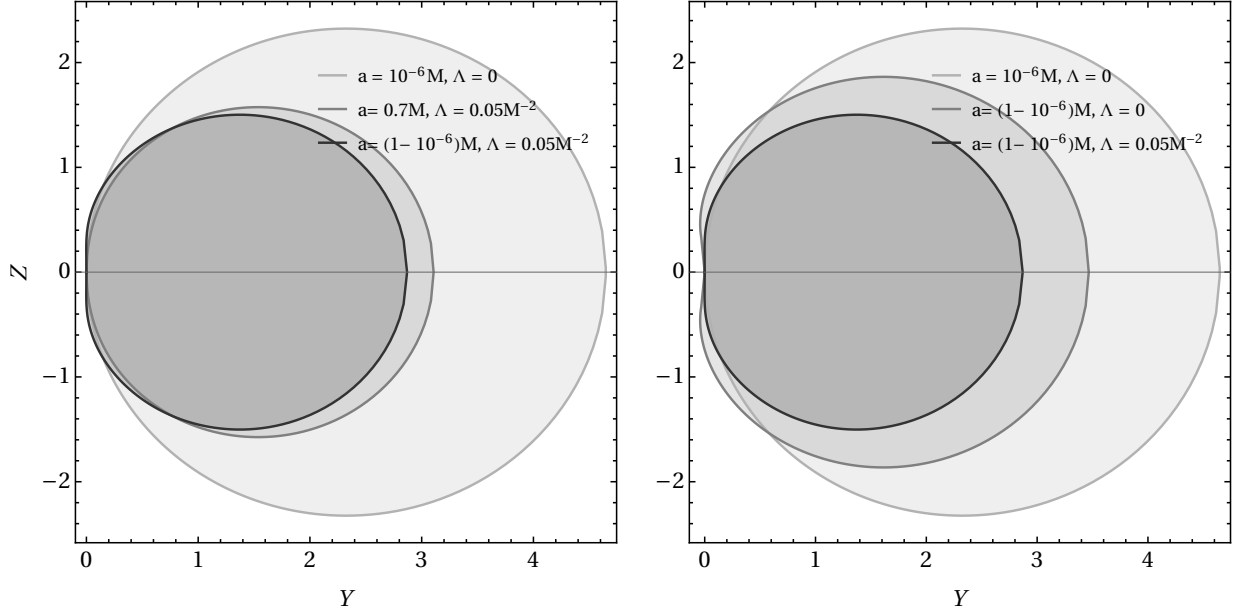


FIG. 9: Shadow of Kerr-de Sitter black holes on projective plane (Y, X) for observers located at $r = 4M$. Left panel: Shadow for Kerr black holes for different spin parameters. Right panel: Shadow for Kerr-de Sitter black holes for different cosmological constant.

of quantity for black hole shadow was firstly proposed by Hioki and Miyamoto [37]. In Figure 10, we plot distortion parameters as function of distance with selected parameters. For Schwarzschild black holes, one can deduce $\delta = 0$. The black hole with the largest spin parameter and smallest cosmological constant has the most distorted shadow. For the rotating black holes, the distortion parameters increases with the distance. It can be understood as part of distortion of shadow attributed to accumulation of propagating effect of light rays. For Kerr-de Sitter black holes, the static observers located beyond cosmological horizon would not observe the shadow any more. And there are not sudden changes of distortion parameter for these observers near the cosmological horizon.

In Figure 11, we plot distortion parameters for observers on cosmological horizon as function of parameters a or Λ . The distortion parameters would increase with spin parameter a and decrease with cosmological constant Λ . The cosmological constant less than $10^{-4}M^{-2}$ doesn't influence much on the distortion parameters of shadow.

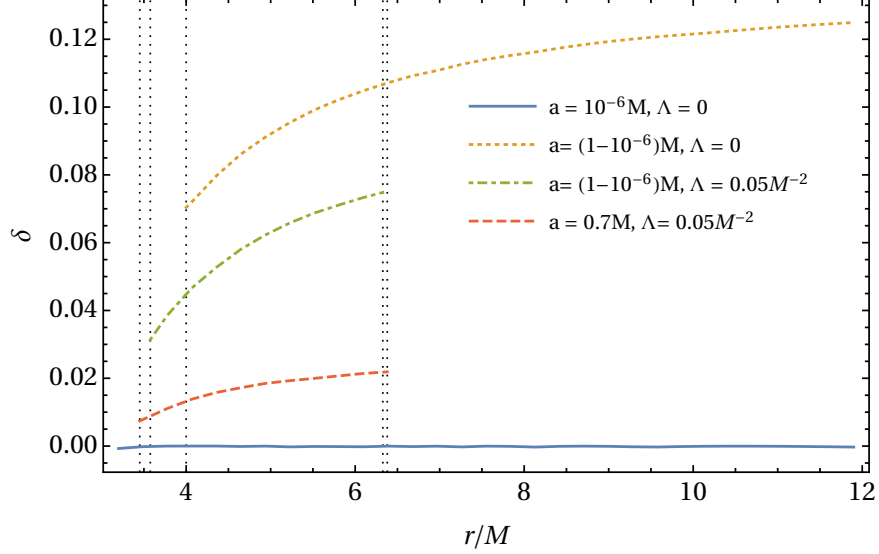


FIG. 10: Distortion parameter as function of distance with selected parameters.

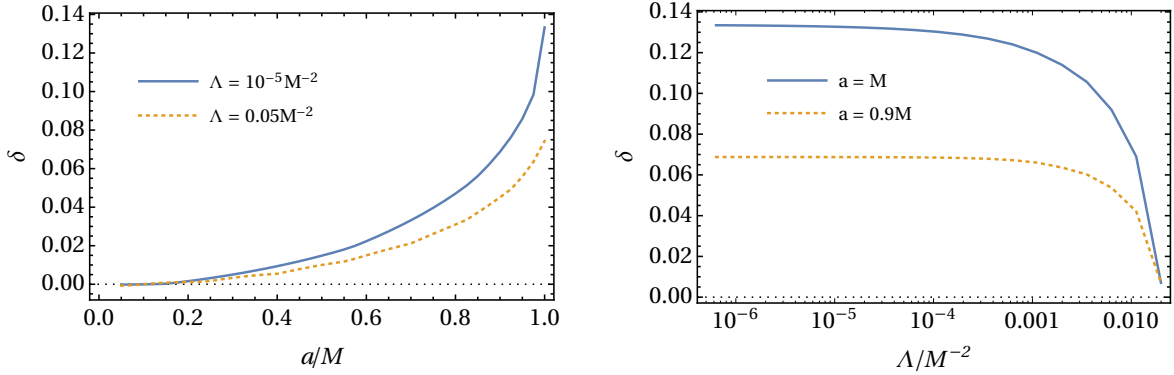


FIG. 11: Left panel: Distortion parameters for observers on cosmological horizon as function of parameters a . Right panel: Distortion parameters for observers on cosmological horizon as function of cosmological constants Λ .

V. COMPARISON WITH ORTHONORMAL TETRAD APPROACHES

We have shown the approach for calculating shadow of rotating black holes without introducing orthonormal tetrad and applied it to Kerr-de Sitter black holes as example. Last but not least, we should compare our results with previous works. Here, we select two representative works of Bardeen [16] and Grenzebach et al. [18]. Their approaches are both suited for studying the shadow with respect to an observer located at finite distance.

In Figure 12, we present shadow of Kerr black holes on projective plane (X, Y) for

observers in large distance and near region, respectively. For the sake of comparison, we use translation and scaling for the results in previous works. As shown in the left panel of Figure 12, the shape of Kerr black hole shadow for distant observers in our approach is exactly the same as that in previous works [16, 18]. In the right panel of Figure 12, Bardeen gave the most distorted shadow among others, while we obtained a shadow with the smallest distortion. We plot distortion parameters as function of distance in these different approaches for Kerr black holes in Figure 13. In large distance, the distortion parameters are exactly the same. In the near region, one might find that Bardeen and Grenzebach et al. gave contrasty results of how the distortion parameter changes with distance. Our results are closed to that obtained by Grenzebach et al.. Namely, the distortion parameter would increase with distance. By the way, one might note that Bardeen’s approach wasn’t equipped with stereographic projection. It suggests that his approach is valid just in tendency for observers located at near region.

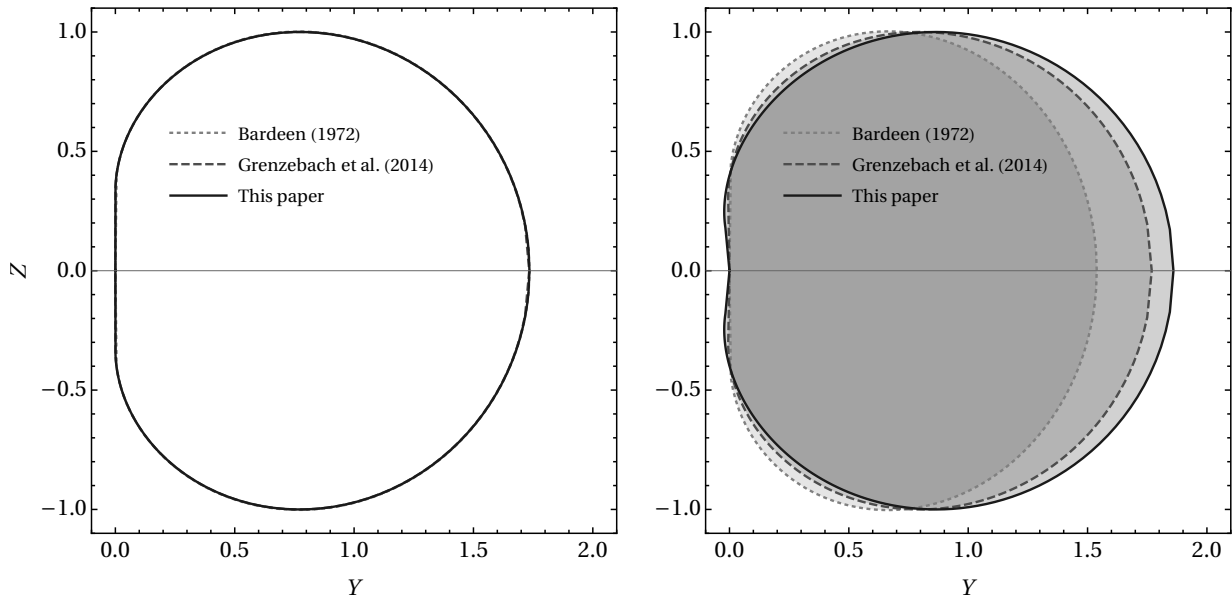


FIG. 12: Scaling shadow of Kerr black holes in different approaches. Left panel: Shadow of Kerr black holes on projective plane (X, Y) for observers located at $r = 40M$. Right panel: shadow of Kerr black holes on projective plane (X, Y) for observers located at $r = 4M$.

For non-asymptotic space-time, we compare our results with Grenzebach et al’s [18]. In Figure 14, we present shadow of Kerr-de Sitter black holes on projective plane (X, Y) for ob-

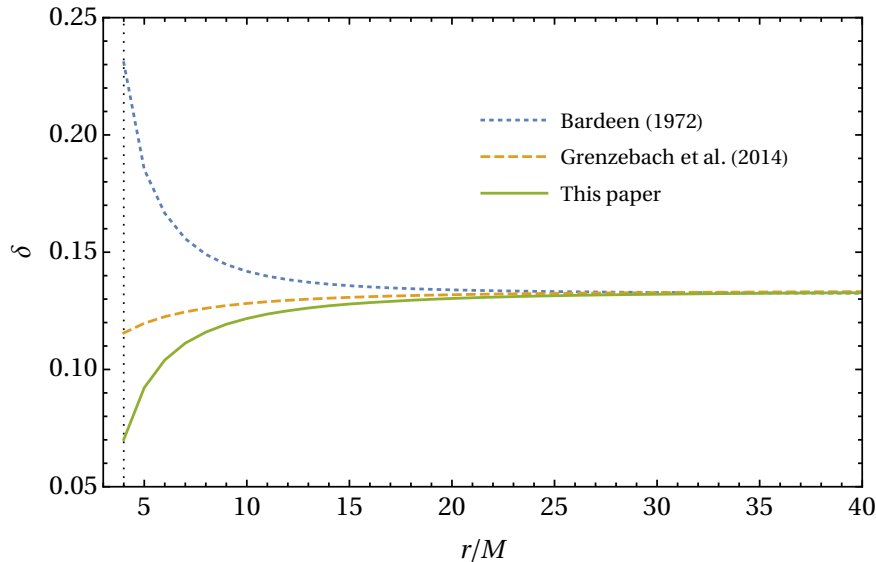


FIG. 13: Distortion parameter as function of distance in different approaches for Kerr black holes.

servers in large distance and near region, respectively. The shadow obtained by Grenzebach et al is more distorted than ours, especially for the observers in near region. In Figure 15, we also compare the distortion parameters as function of distance in these approaches. The distortion parameter of shadow in our approach is smaller and more sensitive to distance. And differed from Kerr black holes, the distortion parameters in different approaches can not be consistent with each other at certain distance.

For those difference shown above, we think there might be two causes. Firstly, the frame of ZAMOs used by Bardeen and Carter's frame used by Grenzebach et al., in fact, suggest the reference frame adapted to different observers. It can be shown via 0-component of these orthonormal tetrads in Kerr space-time [43],

$$(e_0)_{\text{ZAMO}} = \sqrt{\frac{(r^2 + a^2)^2 - a^2 \Delta \sin^2 \theta}{\Delta \Sigma}} \left(\partial_0 + \frac{2aMr}{\sqrt{(r^2 + a^2)^2 - a^2 \Delta \sin^2 \theta}} \partial_3 \right), \quad (58)$$

$$(e_0)_{\text{Carter}} = \frac{r^2 + a^2}{\sqrt{\Delta \Sigma}} \left(\partial_0 + \frac{a}{r^2 + a^2} \partial_3 \right). \quad (59)$$

And neither of them are adapted to a static observer, $u = \frac{1}{\sqrt{-g_{00}}} \partial_0$, which we used in Eqs. (3). In this sense, no one is preferred than others in principle. It's just choice of different reference frame. And all of them are deserved to be considered. Secondly, there is still possibility that our approach with astrometric observables are fundamentally different from the approaches with orthonormal tetrads. To confirm this possibility, further studies are required.

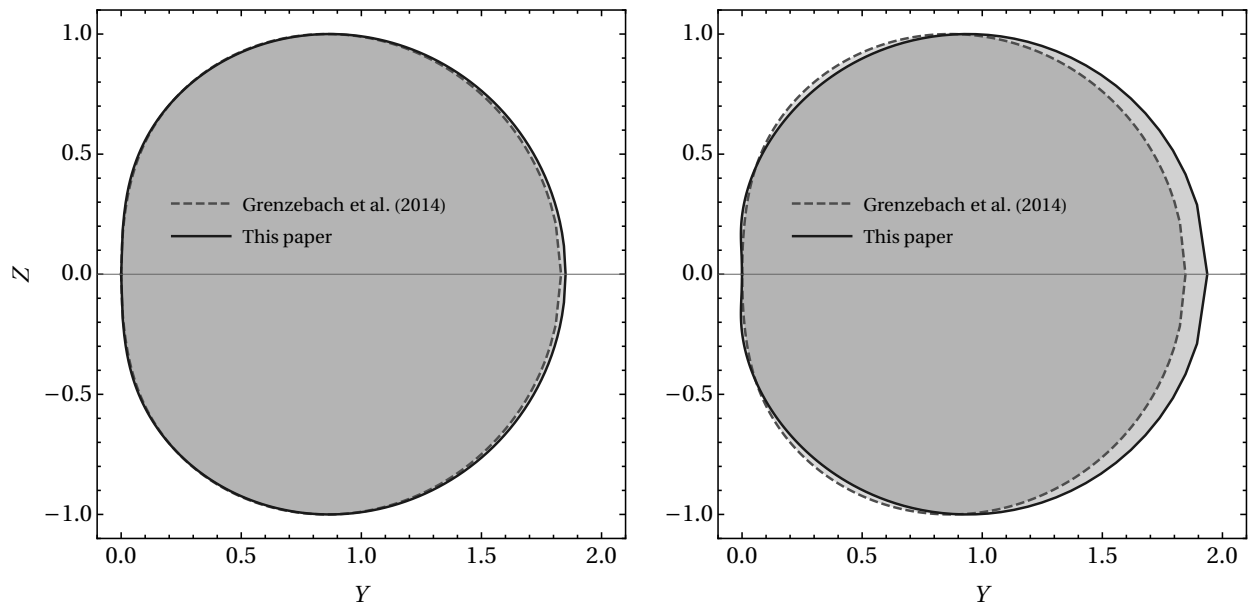


FIG. 14: Shadow of Kerr-de Sitter black holes with cosmological constant $0.05M^{-2}$. Left panel: Shadow of Kerr-de Sitter black holes on projective plane (X, Y) for observers located at cosmological horizon $r \approx 6.31M$. Right panel: Shadow of Kerr-de Sitter black holes on projective plane (X, Y) for observers located at outer boundary of photon region $r \approx 3.57M$

VI. CONCLUSIONS AND DISCUSSIONS

In this paper, we presented a new approach for calculating shadow of rotating black holes with respect to observers at finite distance in formula of astrometric observables. We obtained analytic formulas of a general rotating black hole shadow for given light rays from photon region. With the formulas, we studied size and shape of Kerr-de Sitter black hole shadow as function of distance. In this space-time, we found shadow of Schwarzschild black holes is the biggest and shadow of Kerr black holes is most distorted. For distant observers, our results are consistent with previous works [16, 18]. For near-region observers, our results are closed to Grenzebach et al.'s. Namely, the distortion parameters of shadow would increase with distance.

Here, we only consider static observers fixed at inclination angle $\theta = 0$ and $\theta = \frac{\pi}{2}$. In principle, it can be generalized into arbitrary observers without any technical problems. Namely, one can substitute 4-velocity of observers u in Eqs. (4) or (5) by 4-velocity of

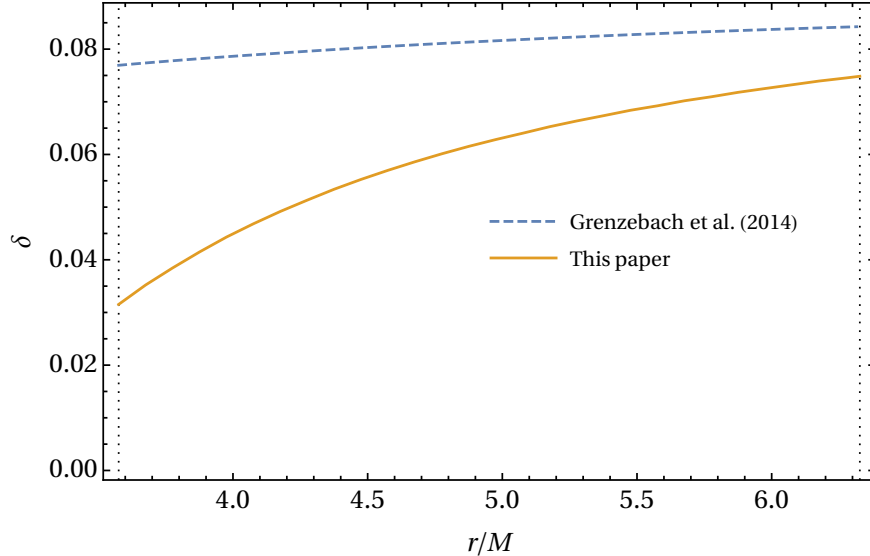


FIG. 15: Distortion parameter as function of distance in different approaches for Kerr-de Sitter black holes.

arbitrary observers.

From studies on shadow of rotating black holes for observers located finite distance, one may get abundant information involving the space-time geometry. Figure 10 might suggest that part distortion of shadow can be attributed to accumulation of propagating effect of light rays. Comparison between previous works with ours in section V suggests that motion status of observers is highly relevant to apparent shape of rotating black holes, especially, for those observers located at finite distance.

ACKNOWLEDGMENTS

This work has been funded by the National Nature Science Foundation of China under grant No. 11675182 and 11690022.

-
- [1] B. P. Abbott *et al.* (LIGO Scientific, Virgo), *Phys. Rev. Lett.* **116**, 241103 (2016), arXiv:1606.04855 [gr-qc].
- [2] T. E. H. T. Collaboration, K. Akiyama, A. Alberdi, W. Alef, K. Asada, R. Azulay, A.-K. Baczko, D. Ball, M. Baloković, J. Barrett, D. Bintley, L. Blackburn, W. Boland, K. L.

Bouman, G. C. Bower, M. Bremer, C. D. Brinkerink, R. Brissenden, S. Britzen, A. E. Broderick, D. Brogiere, T. Bronzwaer, D.-Y. Byun, J. E. Carlstrom, A. Chael, C.-k. Chan, S. Chatterjee, K. Chatterjee, M.-T. Chen, Y. Chen, I. Cho, P. Christian, J. E. Conway, J. M. Cordes, G. B. Crew, Y. Cui, J. Davelaar, M. D. Laurentis, R. Deane, J. Dempsey, G. Desvignes, J. Dexter, S. S. Doeleman, R. P. Eatough, H. Falcke, V. L. Fish, E. Fomalont, R. Fraga-Encinas, P. Friberg, C. M. Fromm, J. L. Gómez, P. Galison, C. F. Gammie, R. García, O. Gentaz, B. Georgiev, C. Goddi, R. Gold, M. Gu, M. Gurwell, K. Hada, M. H. Hecht, R. Hesper, L. C. Ho, P. Ho, M. Honma, C.-W. L. Huang, L. Huang, D. H. Hughes, S. Ikeda, M. Inoue, S. Issaoun, D. J. James, B. T. Jannuzi, M. Janssen, B. Jeter, W. Jiang, M. D. Johnson, S. Jorstad, T. Jung, M. Karami, R. Karuppusamy, T. Kawashima, G. K. Keating, M. Kettenis, J.-Y. Kim, J. Kim, J. Kim, M. Kino, J. Y. Koay, P. M. Koch, S. Koyama, M. Kramer, C. Kramer, T. P. Krichbaum, C.-Y. Kuo, T. R. Lauer, S.-S. Lee, Y.-R. Li, Z. Li, M. Lindqvist, K. Liu, E. Liuzzo, W.-P. Lo, A. P. Lobanov, L. Loinard, C. Lonsdale, R.-S. Lu, N. R. MacDonald, J. Mao, S. Markoff, D. P. Marrone, A. P. Marscher, I. Martí-Vidal, S. Matsushita, L. D. Matthews, L. Medeiros, K. M. Menten, Y. Mizuno, I. Mizuno, J. M. Moran, K. Moriyama, M. Moscibrodzka, C. Müller, H. Nagai, N. M. Nagar, M. Nakamura, R. Narayan, G. Narayanan, I. Natarajan, R. Neri, C. Ni, A. Noutsos, H. Okino, H. Olivares, T. Oyama, F. Özel, D. C. M. Palumbo, N. Patel, U.-L. Pen, D. W. Pesce, V. Piétu, R. Plambeck, A. Pop-Stefanija, O. Porth, B. Prather, J. A. Preciado-López, D. Psaltis, H.-Y. Pu, V. Ramakrishnan, R. Rao, M. G. Rawlings, A. W. Raymond, L. Rezzolla, B. Ripperda, F. Roelofs, A. Rogers, E. Ros, M. Rose, A. Roshanineshat, H. Rottmann, A. L. Roy, C. Ruszczyk, B. R. Ryan, K. L. J. Rygl, S. Sánchez, D. Sánchez-Arguelles, M. Sasada, T. Savolainen, F. P. Schloerb, K.-F. Schuster, L. Shao, Z. Shen, D. Small, B. W. Sohn, J. SooHoo, F. Tazaki, P. Tiede, R. P. J. Tilanus, M. Titus, K. Toma, P. Torne, T. Trent, S. Trippe, S. Tsuda, I. v. Bemm, H. J. v. Langevelde, D. R. v. Rossum, J. Wagner, J. Wardle, J. Weintroub, N. Wex, R. Wharton, M. Wielgus, G. N. Wong, Q. Wu, A. Young, K. Young, Z. Younsi, F. Yuan, Y.-F. Yuan, J. A. Zensus, G. Zhao, S.-S. Zhao, Z. Zhu, J. R. Farah, Z. Meyer-Zhao, D. Michalik, A. Nadolski, H. Nishioka, N. Pradel, R. A. Primiani, K. Souccar, L. Vertatschitsch, and P. Yamaguchi, *Astrophys. J. Lett.* **875**, L6 (2019).

- [3] C. Goddi, H. Falcke, M. Kramer, L. Rezzolla, C. Brinkerink, T. Bronzwaer, J. R. J. Davelaar, R. Deane, M. De Laurentis, G. Desvignes, R. P. Eatough, F. Eisenhauer, R. Fraga-Encinas,

- C. M. Fromm, S. Gillessen, A. Grenzebach, S. Issaoun, M. Janßen, R. Konoplya, T. P. Krichbaum, R. Laing, K. Liu, R.-S. Lu, Y. Mizuno, M. Moscibrodzka, C. Müller, H. Olivares, O. Pfuhl, O. Porth, F. Roelofs, E. Ros, K. Schuster, R. Tilanus, P. Torne, I. van Bemmell, H. J. van Langevelde, N. Wex, Z. Younsi, and A. Zhidenko, *Int. J. Mod. Phys. D* **26**, 1730001 (2016).
- [4] J. L. Synge, *Mon. Not. R. Astron. Soc.* **131**, 463 (1966).
- [5] M. Wang, S. Chen, and J. Jing, *Phys. Rev. D* **97**, 064029 (2018).
- [6] S. X. Tian and Z.-H. Zhu, *Phys. Rev. D* **100**, 064011 (2019).
- [7] R. A. Konoplya, *Phys. Lett. B* **795**, 1 (2019).
- [8] T. Zhu, Q. Wu, M. Jamil, and K. Jusufi, *Phys. Rev. D* **100**, 044055 (2019), arXiv: 1906.05673.
- [9] A. Allahyari, M. Khodadi, S. Vagnozzi, and D. F. Mota, *J. Cosmol. Astropart. Phys.* **2020** (02), 003, arXiv: 1912.08231.
- [10] V. Perlick, O. Y. Tsupko, and G. S. Bisnovaty-Kogan, *Phys. Rev. D* **97**, 104062 (2018).
- [11] G. S. Bisnovaty-Kogan and O. Y. Tsupko, *Phys. Rev. D* **98**, 084020 (2018).
- [12] O. Y. Tsupko and G. S. Bisnovaty-Kogan, arXiv:1912.07495 [gr-qc] (2019), arXiv: 1912.07495.
- [13] J. T. Firouzjaee and A. Allahyari, *Eur. Phys. J. C* **79**, 10.1140/epjc/s10052-019-7464-2 (2019).
- [14] Z. Chang and Q.-H. Zhu, (2019), arXiv:1911.02190 [gr-qc].
- [15] S. Vagnozzi, C. Bambi, and L. Visinelli, *Class. Quantum Grav.* 10.1088/1361-6382/ab7965 (2020), arXiv: 2001.02986.
- [16] J. M. Bardeen, in *Proceedings, Ecole d'Et de Physique Thorique: LesAstres Occlus: Les Houches, France, August, 1972* (1973) pp. 215–239.
- [17] H. Falcke, F. Melia, and E. Agol, *Astrophys. J. Lett.* **528**, L13 (1999).
- [18] A. Grenzebach, V. Perlick, and C. Lämmerzahl, *Phys. Rev. D* **89**, 124004 (2014).
- [19] Z. Stuchlík, D. Charbulák, and J. Schee, *Eur. Phys. J. C* **78**, 180 (2018).
- [20] P.-C. Li, M. Guo, and B. Chen, (2020), arXiv:2001.04231 [gr-qc].
- [21] F. Atamurotov, A. Abdujabbarov, and B. Ahmedov, *Phys. Rev. D* **88**, 064004 (2013).
- [22] Z. Li and C. Bambi, *J. Cosmol. Astropart. Phys.* **2014** (01), 041.
- [23] A. Abdujabbarov, M. Amir, B. Ahmedov, and S. G. Ghosh, *Phys. Rev. D* **93**, 104004 (2016).
- [24] C. Bambi, K. Freese, S. Vagnozzi, and L. Visinelli, *Phys. Rev. D* **100**, 044057 (2019), arXiv: 1904.12983 version: 2.

- [25] A. Grenzebach, V. Perlick, and C. Lämmerzahl, *Int. J. Mod. Phys. D* **24**, 1542024 (2015).
- [26] S. Vagnozzi and L. Visinelli, *Phys. Rev. D* **100**, 024020 (2019), arXiv: 1905.12421.
- [27] I. Banerjee, S. Chakraborty, and S. SenGupta, *Phys. Rev. D* **101**, 041301 (2020), arXiv: 1909.09385.
- [28] K. Jusufi, M. Jamil, P. Salucci, T. Zhu, and S. Haroon, *Phys. Rev. D* **100**, 044012 (2019).
- [29] P. V. P. Cunha, C. A. R. Herdeiro, E. Radu, and H. F. Rúnarsson, *Phys. Rev. Lett.* **115**, 211102 (2015).
- [30] P. V. P. Cunha, C. A. R. Herdeiro, and E. Radu, *Universe* **5**, 220 (2019), arXiv: 1909.08039.
- [31] S. Haroon, M. Jamil, K. Jusufi, K. Lin, and R. B. Mann, *Phys. Rev. D* **99**, 044015 (2019).
- [32] S.-W. Wei, Y.-X. Liu, and R. B. Mann, *Phys. Rev. D* **99**, 041303 (2019).
- [33] N. Bar, K. Blum, T. Lacroix, and P. Pani, *J. Cosmol. Astropart. Phys.* **2019** (07), 045, arXiv: 1905.11745.
- [34] H. Davoudiasl and P. B. Denton, *Phys. Rev. Lett.* **123**, 021102 (2019), arXiv: 1904.09242.
- [35] R. Roy and U. A. Yajnik, *Phys. Lett. B* **803**, 135284 (2020), arXiv: 1906.03190.
- [36] C. Li, S.-F. Yan, L. Xue, X. Ren, Y.-F. Cai, D. A. Easson, Y.-F. Yuan, and H. Zhao, arXiv:1912.12629 [astro-ph, physics:gr-qc, physics:hep-th] (2019), arXiv: 1912.12629.
- [37] K. Hioki and U. Miyamoto, *Phys. Rev. D* **78**, 044007 (2008).
- [38] K. Hioki and K.-i. Maeda, *Phys. Rev. D* **80**, 024042 (2009).
- [39] T. Johannsen, *Astrophys. J.* **777**, 170 (2013), arXiv: 1501.02814.
- [40] A. A. Abdujabbarov, L. Rezzolla, and B. J. Ahmedov, *Mon. Not. R. Astron. Soc.* **454**, 2423 (2015).
- [41] A. Övgün, İ. Sakallı, and J. Saavedra, *J. Cosmol. Astropart. Phys.* **2018** (10), 041, arXiv: 1807.00388.
- [42] R. Kumar, S. G. Ghosh, and A. Wang, *Phys. Rev. D* **100**, 124024 (2019).
- [43] D. Bini, A. Geralico, and R. T. Jantzen, *Phys. Rev. D* **95**, 124022 (2017), arXiv: 1703.09525.
- [44] E. F. Eiroa and C. M. Sendra, *Eur. Phys. J. C* **78**, 10.1140/epjc/s10052-018-5586-6 (2018).
- [45] M. H. Soffel and W.-B. Han, *Applied General Relativity* (Springer, 2019).
- [46] D. Lebedev and K. Lake, arXiv:1308.4931 [gr-qc] (2013), arXiv: 1308.4931.
- [47] C. T. Cunningham, *Phys. Rev. D* **12**, 323 (1975).
- [48] Z. Stuchlík and K. PišKová, *RAGtime 4/5: Workshops on black holes and neutron stars*, 167 (2004).

[49] R. A. Konoplya and A. Zhidenko, *Rev. Mod. Phys.* **83**, 793 (2011).